J. Physiol. (1977), **268**, *pp.* 575–611
With 15 text-figures
Printed in Great Britain

REGENERATIVE REPOLARIZATION OF THE FROG VENTRICULAR ACTION POTENTIAL: A TIME AND VOLTAGE-DEPENDENT PHENOMENON

BY YALE GOLDMAN AND MARTIN MORAD

From the Department of Physiology, University of Pennsylvania, Philadelphia, Pennsylvania 19174, U.S.A.

(*Received 2 September 1975*)

SUMMARY

1. The regenerative repolarization process has been examined in frog ventricular myocardium using a single sucrose gap voltage clamp technique.

2. Application of brief (30–150 msec) anodal voltage clamp pulses during the plateau of the action potential revealed a 'threshold' potential region for immediate repolarization. The response to anodal clamp pulses was not all-or-none but was graded.

3. The threshold potential was strongly dependent on the duration of the test voltage clamp pulses and was more negative for shorter clamps.

4. Regenerative repolarization was also observed in the presence of tetrodotoxin.

5. No threshold for immediate repolarization was observed with very short clamps (2–20 msec in duration). Instead the membrane depolarized upon release of each clamp pulse.

6. Theoretical and experimental analysis of the potential distribution in the preparations showed that the de- and repolarizations observed after test clamp steps are not due to geometrical properties or inhomogeneous potential distributions.

7. The results suggest that the instantaneous I–V relation of the membrane during the plateau may be linear.

INTRODUCTION

Several electrophysiological studies of the heart action potential have indicated that initiation of the rapid repolarization phase is a regenerative process. Weidmann (1951) and Vassalle (1966) in sheep Purkinje fibres and Cranefield & Hoffman (1958) in dog and cat papillary muscles demonstrated a threshold for immediate repolarization between the plateau and

resting potentials. The possible ionic mechanisms considered for the rapid repolarization were a regenerative decrease of the Na^+ and/or Ca^{2+} permeability or an increase of K^+ permeability. An experimental approach to distinguish between these possibilities was to measure the total membrane conductance during the action potential. Weidmann (1951) had obtained values for membrane slope conductance during the action potential and at rest by measuring the voltage deflexion resulting from application of 70 msec transmembrane current pulses. He found that the membrane conductance in the plateau was not only lower than at rest but decreased further toward the end of the plateau. One interpretation of these results is that during the plateau the Na^+ and Ca^{2+} permeabilities are low and that the K^+ permeability is even lower than its resting value. If the instantaneous I–V relation of the membrane were fairly linear, then the decrease of conductance toward the end of the plateau would indicate a decrease in Na^+ and/or Ca^{2+} permeabilities to initiate the rapid repolarization (Brady & Woodbury, 1960). On the other hand, rapid time-dependent permeability changes might occur during the pulses so that the effective I–V relation is N-shaped. Then the threshold and slope conductance results would be consistent with an increase in K^+ permeability to rapidly terminate the plateau (Noble, 1962*a*). Both of these interpretations depended on the assumption that the permeability change primarily responsible for the rapid repolarization is much slower than the applied current pulses. Further, the apparent 'threshold' phenomenon might not be an intrinsic property of the sarcolemma and might occur only as a result of conduction and spacial potential gradients in the syncytial myocardium.

In this and the following papers we have re-examined the regenerative repolarization process of the plateau using a modified single sucrose gap voltage clamp technique (Morad & Orkand, 1971; Beeler & Reuter, 1970). Frog ventricular myocardium was used because this preparation lacks T-tubules or deep intracellular clefts (Staley & Benson, 1968; Sommer & Johnson, 1969; Page & Niedergerke, 1972) and its action potential has a prominent plateau. The plateau was interrupted by voltage clamp pulses of varying durations and test potentials. The membrane current during the clamps as well as the time course of membrane potential subsequent to termination of the clamps were measured. Experiments were conducted in the presence and absence of tetrodotoxin to determine the contribution of the rapid Na^+ transport system (Hagiwara & Nakajima, 1966; Dudel, Peper, Rüdel & Trautwein, 1967) to the regenerative repolarization process. Analysis of the spacial potential distribution in the muscle was made to distinguish between the intrinsic electrical properties of the membrane and inhomogeneity of current and voltage distributions. These experiments showed that the threshold for immediate repolarization was

not a unique potential, but depended on the duration of test clamp. The results suggest that the instantaneous $I-V$ relation of the membrane has no negative conductance region and may be, in fact, linear.

A preliminary report of these findings has been presented (Goldman & Morad, 1973).

METHODS

Quiescent strips 500 μm or less in diameter were dissected from the basal region of the ventricle of frogs (*Rana pipiens*). The strip was placed in a single sucrose gap voltage clamp apparatus similar to that described by Morad & Orkand (1971). The muscle was drawn through 300 μm holes in two latex membranes (thickness 50 μm) which separated the ventricular strip into three independently perfused compartments. The length of the muscle in the physiological (Ringer) pool was less than 0·5 mm. A standard 3 M-KCl-filled glass micro-electrode was used to record intracellular potential of the muscle in the Ringer pool. This potential was fed back through a high gain inverting amplifier which applied current across the sucrose gap via Ag/AgCl electrodes to clamp the membrane potential of the muscle in the Ringer pool. The potential outside the muscle in the Ringer pool was 'ground clamped' by a separate circuit. The current required to hold the extracellular potential at ground during the clamp was measured and taken as net membrane current (Morad & Orkand, 1971; Goldman & Morad, 1977*a*). The end of the muscle was tied to a semiconductor strain gauge (Endevco S8 107–2) for isometric tension measurement.

Solutions. The three compartments were perfused with solutions of the following composition in m-mole/l. (*a*) physiological Ringer pool: NaCl, 116; KCl, 3; $NaHCO_3$, 2; $CaCl_2$, 0·2; (*b*) central sucrose compartment; sucrose, 210 (special enzyme grade, Schwarz-Mann); $MnSO_4$, 0·01 (added in some experiments as a contractile suppressant for the muscle in the central compartment); (*c*) KCl pool: KCl, 120; $NaHCO_3$, 2. All solutions were prepared with deionized double-distilled water. In some experiments tetrodotoxin, 5×10^{-7}–10^{-6} mole/l (Sigma), was added to the normal Ringer solution.

Stimulation. The ventricular strip was stimulated 12 times/min by a 5 msec current pulse passed between KCl and Ringer pools. After termination of the pulse, the KCl electrode was electronically disconnected from the stimulator by a low leakage ($< 10^{-9}$A) field effect transistor. This allowed accurate measurement of the potential between the KCl and the Ringer pools during an action potential and immediately after termination of a voltage clamp step. The transgap potential was monitored continuously and was used to determine the spacial potential distribution in the muscle (see Results).

Tests and precautions. A major segment of this report deals directly with the adequacy of the spacial clamp of voltage and current distributions in the single sucrose gap. By comparing experimental measurements of the spacial potential distributions with those predicted by an idealized cable model suggested by Sir Alan Hodgkin for the case of single sucrose gap necessary criteria for artifact-free results were derived. These criteria are as follows: (1) the physiological node must be small (< 500 μm in length and diameter; see Morad & Orkand, 1971); (2) the electrode must be placed half way between the sucrose gap and the end of the muscle tied to the tension transducer in the Ringer pool; (3) the currents accompanying repolarizing clamp pulses from the plateau must be free of 'abominable notches' and transient inward current bumps; (4) the recorded current during an anodal voltage clamp

pulse must be initially inward and decrease monotonically toward outward current during the clamp step; and (5) the direction of membrane polarization immediately following a clamp pulse must be strictly related to the sign of the membrane current at the end of the clamp, i.e. inward final clamp current must result in depolarization and outward final clamp current must be followed by repolarization.

In addition to application of these criteria, the general procedure was to place the muscle in the sucrose gap chamber and stimulate it for about one hour before the

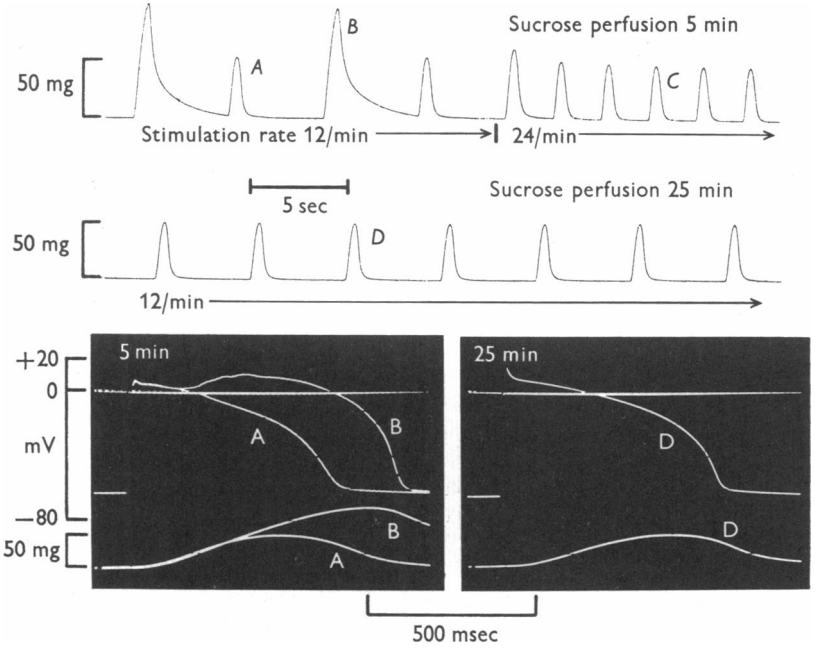

Fig. 1. Transgap action potentials and accompanying contractions recorded from a ventricular strip during the initial period of perfusion in a sucrose gap chamber. Traces *A* and *B*, alternating regular and aberrant action potentials and contractions recorded 5 min after the start of sucrose perfusion. Stimulation rate, 12/min. Alternans ceases at stimulation rate of 24/min (trace *C*). After 25 min of sucrose perfusion, action potentials and accompanying contractions appear normal at both stimulation rates (trace *D* stimulation rate, 12/min). 15–40 min are required to eliminate excitability of cells in the sucrose gap.

start of the experiment to allow for equilibration and 'healing' (De Mello, 1972). The transgap action potentials recorded in the initial period of perfusion often appeared 'bumpy' and prolonged. Fig. 1 shows recordings of transgap action potentials and the accompanying contractions 5 min after the start of perfusion. Alternating 'bumpy' and smooth action potentials such as shown in traces *A* and *B* were often recorded. The contractions accompanying the irregular action potentials (trace *B*) were large, prolonged and slowly relaxing. During this time, the extracellular space of the muscle in the sucrose gap was probably not sufficiently ex-

changed to eliminate excitability in that region of the muscle or at the Ringer-sucrose interface. Under these conditions, when the frequency of stimulation was doubled to 24/min (twitches labelled *C*), the electrical and mechanical alternans ceased and all the action potentials became regular. The contractions were uniform and relaxation was rapid. This suggests that the irregularities at the lower rate were due to marginally excitable cells with a long refractory period.

After 15–40 min of sucrose perfusion, the action potential recorded across the sucrose gap became similar to an intracellularly recorded action potential at all frequencies of stimulation (trace *D*). A transgap action potential magnitude of 70–100 mV and 500–800 msec in duration was required to begin the experiment.

An intracellular micropuncture near the centre of physiological node was then obtained with a stable resting potential of −75 to −85 mV and action potential

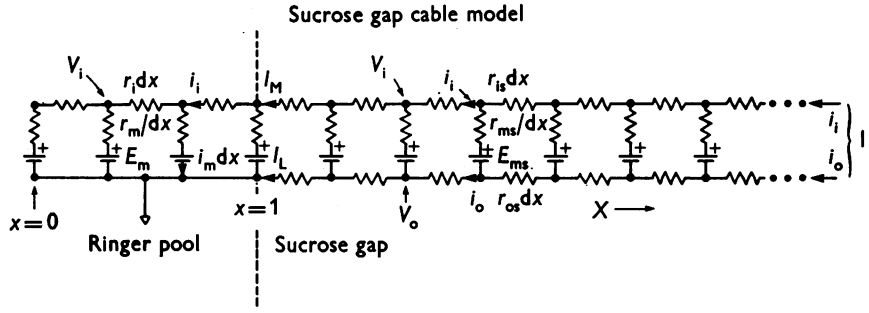

Fig. 2. Idealized longitudinal electrical equivalent of a ventricular strip in the sucrose gap chamber. The extracellular longitudinal resistivity (r_{os}) is assumed to be much higher in the sucrose region than in the Ringer pool. Intracellular resistivity (r_i), membrane resistivity (r_m) and membrane equilibrium potential (E_m) are allowed to differ in Ringer and sucrose compartments. The intracellular (V_i) and extracellular (V_o) potentials are calculated in the Appendix. The model predicts longitudinal potential gradients in the muscle according to the direction of the applied current.

overshoot of +15 to +25 mV. About 50–75 % of the preparations were unacceptable by the above criteria and were eliminated from consideration of physiological results.

Theory

Since the validity of the voltage clamp results to be described will depend on the homogeneity of the distribution of potential in various regions of the physiological node, it is of interest to consider the distribution of potential expected on a theoretical basis. An idealized and highly simplified model of the longitudinal electrical cable structure of the ventricular muscle in the sucrose gap is shown in Fig. 2. The model is similar to that suggested by Sir Alan Hodgkin (see McGuigan, 1974, for the case of the double sucrose gap). In this model the longitudinal internal and membrane resistivities in the sucrose region are allowed to differ from the corresponding parameters in the Ringer pool. The fundamental characteristic of the muscle in the single or double sucrose gap models is that the longitudinal extracellular resistivity is considerably higher in the sucrose than in the Ringer region.

The formal assumptions made in this model are: (*a*) linear and passive longitudinal and membrane resistivities; (*b*) steady-state current and potential distributions;

(*c*) no longitudinal current flow from the end of the strip in the Ringer pool (an open-circuit termination); (*d*) greater extracellular longitudinal resistivity in sucrose than in Ringer pools; (*e*) a negligible extracellular potential in Ringer pool; (*f*) negligible radial potential gradients in the muscle; (*g*) negligible mixing of solutions at the Ringer–sucrose interface; and (*h*) length of the sucrose gap considerably greater than the longitudinal space constant in the sucrose region.

Although many of these assumptions are not experimentally justified, they define a model which is mathematically explicit and is a rough first approximation of the longitudinal cable properties of the muscle. The intracellular and extracellular potentials are functions of distance and are derived in the appendix. They are given by

$$V_o = \begin{cases} 0 & 0 \leqslant x \leqslant 1 \\ \dfrac{(V_1 - E_{ms})r_{os}}{r_{is}+r_{os}}\,(1-e^{(x-1)/\lambda}s) + r_p I(x-l); & 1 \leqslant x \leqslant \infty \end{cases} \tag{1.14}$$

$$V_i = \begin{cases} E_m + (V_1 - E_m)\dfrac{\cosh(x/\lambda)}{\cosh(1/\lambda)} & 0 \leqslant x \leqslant 1 \\ \dfrac{V_1 r_o + E_{ms} r_{is}}{r_{is}+r_{os}} + \dfrac{(V_1 - E_{ms})r_{is}}{r_{is}+r_{os}}\,e^{-(x-1)/\lambda_s} + r_p I(x-l) & 1 \leqslant x \leqslant \infty, \end{cases} \tag{1.9, 1.15}$$

where V_i = intracellular potential (V), V_o = extracellular potential (V), V_m = transmembrane potential, $V_i - V_o$ (V), V_1 = transmembrane potential at Ringer sucrose interface (V), V_e = transmembrane potential at the end of the muscle ($x = 0$) (V), V_g = potential of the KCl pool with respect to the Ringer pool, the transgap potential (V), E_m, E_{ms} = membrane equilibrium potential in the Ringer and sucrose regions respectively (V), x = distance from the end of the muscle (cm), l = length of the muscle in the Ringer pool (cm), r_m, r_{ms} = membrane resistivity in Ringer and sucrose regions respectively (Ω – cm), r_i, r_{is} = longitudinal internal resistivity in Ringer and sucrose regions respectively (Ω/cm), r_{os} = longitudinal external resistivity in the sucrose region (Ω/cm), r_p = longitudinal resistivity of the preparation in the sucrose region, $r_{is} \cdot r_{os}/(r_{is}+r_{os})$ (Ω/cm), i_m = membrane current density; positive current flows outward through r_m (A/cm), i_i, i_o = longitudinal internal and external current respectively, positive current flows in the sucrose-to-Ringer direction (A), I = total applied longitudinal current; $i_i + i_o$ (A), I_m = total membrane current in the Ringer solution (A), I_L = leakage current (A).

Eqns. (1.9), (1.14) and (1.15) are plotted in Fig. 3 for three cases of transgap current flow. E_{ms} is assumed to be zero in Fig. 3. For case *A*, no applied current, the transgap potential (V_g) is an attenuated version of the intracellular potential at the Ringer-sucrose interface (V_1) and is given by

$$V_g = \frac{V_1 r_{os}}{r_{is}+r_{os}} \quad \text{(see also Morad \& Orkand, 1971).} \tag{1.16}$$

For case *B*, outward applied current (positive I), the longitudinal current flow is in the sucrose-to-Ringer direction and, therefore, the intracellular potential gradient is in the sucrose-to-Ringer direction. For case *C*, inward applied current (negative I), the longitudinal current flows in the opposite direction and the intracellular potential gradient is in the Ringer-to-sucrose direction. These theoretically predicted potential gradients are compared in the Results section with experimentally measured potential gradients in ventricular strips during voltage clamps in the single sucrose gap apparatus.

RESULTS

Properties of regenerative repolarization

Plateau position and voltage-dependent repolarization. The plateau of a ventricular action potential was interrupted by repolarizing the membrane to different potentials with brief voltage clamp steps. In Fig. 4*A*, the resting potential (lower left trace) and upstroke (upper left trace) of an

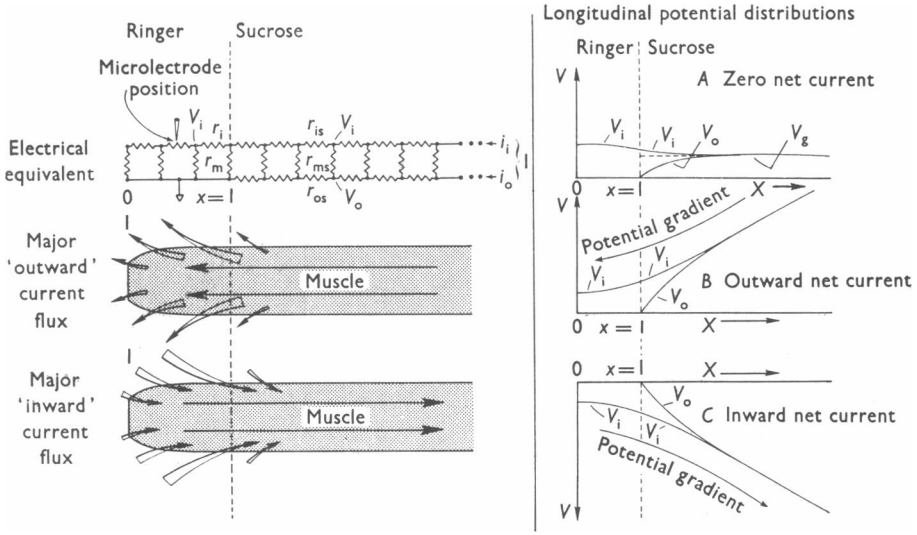

Fig. 3. Predictions of the idealized cable model of voltage distributions during application of current through the sucrose gap. The membrane equilibrium potential of the sucrose gap (E_{ms} of Fig. 2) has been assumed to be the same as the resting potential of the muscle in the Ringer pool in this figure. The intracellular (V_i) and extracellular (V_o) potentials are plotted as the difference from resting potential versus distance. Case *A* (zero net current), the potential in the transgap position (V_g) and is an attenuated version of the intracellular potential (V_i) at the Ringer–sucrose interface. Case *B*, during application of outward net current, the intracellular current flows in the sucrose-to-Ringer (i.e. right-to-left) direction. This results in an intracellular potential gradient in the sucrose-to-Ringer direction. Case *C*, during application of inward net current, the intracellular current flows in the Ringer-to-sucrose direction (i.e. left-to-right). This results in an intracellular potential gradient in the Ringer-to-sucrose direction.

action potential are shown. At 50 msec after the stimulus, the plateau was repolarized to -32 mV for 85 msec and then the clamp pulse was terminated. Upon release of the clamp, the membrane depolarized to nearly plateau potential and then finally repolarized. During the plateau of a

subsequent beat, the membrane was repolarized to −37 mV for 85 msec and then released. The records of two interrupted action potentials have been superimposed in Fig. 4*A*. Upon release of the more negative clamp, the membrane immediately repolarized. With clamps of such durations

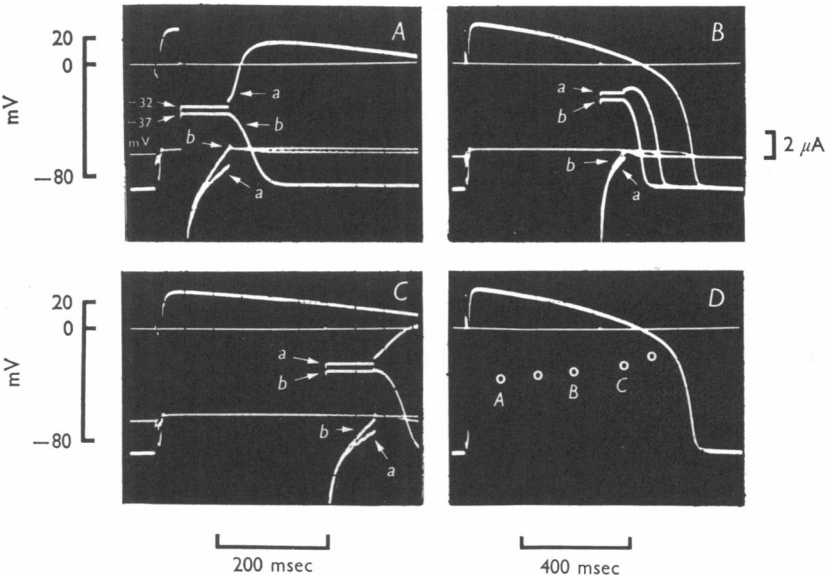

Fig. 4. Measurement of the 'apparent threshold' of repolarization for 85 msec voltage clamp pulses applied at various times during the plateau. Preparation was stimulated 12 shocks/min. Clamp pulses were applied during every second action potential. Upper traces, membrane potential. Lower traces, uncompensated voltage clamp currents. Inward current is plotted downward. Outward current is plotted upward. Panels *A*, *B*, and *C*, super-imposed records of two voltage clamp pulses differing in potential by 5 mV. The clamps were initiated 50, 300 and 480 msec after the stimulus. Panel *D*, the apparent 'threshold' potential for immediate repolarization is plotted for 85 msec test clamps versus the time after the stimulus of clamp termination. The threshold potential slowly rises during the plateau. The small deflexions of the current trace during non-voltage clamp conditions are due to sucrose gap leakage current and operation of the 'leakage clamp' mode of the sucrose gap apparatus (Goldman & Morad, 1977*a*).

a critical potential was observed (in Fig. 4*A* between −32 and −37 mV) above which the membrane depolarized upon release and below which the membrane immediately repolarized.

The value of this critical potential depends on the amount of time the membrane was at the plateau potential before the clamp was applied.

Fig. 4*B* and *C* show similar measurements at later times during the plateau. The critical potential for immediate repolarization after 85 msec clamp steps is plotted vs the time of termination of the clamp within the plateau (Fig. 4*D*). The 'threshold' potential slowly becomes less negative during the time course of the plateau and seems to intersect the action potential near the beginning of the rapid phase of repolarization. Thus, as the membrane slowly repolarizes during the plateau, the critical potential for the onset of rapid repolarization rises, so that when the action potential and the critical potential intersect the rapid repolarization occurs.

The 'uncompensated' membrane currents required to clamp the potentials have been included in Fig. 4*A*, *B*, and *C* as the lower trace. Note that when the current at the end of the clamp is inward (plotted downward), the membrane depolarizes upon release of the clamp and when the final clamp current is outward the membrane immediately repolarizes (see section, 'Clamp currents during development of regenerative repolarization' for a more detailed description of the current records).

Time-dependent repolarization. Fig. 5 shows a normal action potential superimposed upon two subsequent plateaus which were interrupted by voltage clamp steps. The clamps were applied to the same potential and ended at the same time after the stimulus. However, the clamps were initiated at different times in the plateau as is indicated by the arrows and the membrane current traces (upper traces), and so are of different durations. Release of the shorter clamp resulted in depolarization toward the plateau potential and the longer clamp pulse caused immediate repolarization. This observation suggests that no unique threshold potential for immediate repolarization exists but that the rapid repolarization effect is dependent on both the duration and the potential of the clamp. The uncompensated membrane current recorded during the shorter clamp (upper trace) was initially inward and was still inward at the end of the clamp which resulted in depolarization. On the other hand, the current at the end of the clamp which caused repolarization was outward.

It might be argued that the time of initiation of the clamps in Fig. 5 rather than the duration of the pulse determines the subsequent time course of the membrane potential. This possibility was tested by comparing clamps of various durations applied at different times in the plateau. Fig. 6, panels *A*, *C*, and *E* show series of clamps of different durations (85, 130, and 170 msec) which all *started* 160 msec after stimulus. Panels *B*, *D*, and *E* show clamps of differing durations (85, 130 and 170 msec) which all *ended* at 330 msec after the stimulus. In each case longer clamps resulted in a less negative threshold potential whether the clamps started at equivalent times (e.g. compare panels *C* and *E*) or ended at equivalent times (e.g. compare *D* and *E*). Clearly, it is the duration rather

than just the position of the clamp in the plateau which strongly influences the critical potential for immediate repolarization.

The interaction between the duration and the position of the clamp pulses during the plateau on the threshold potential is shown in Fig. 7. Panels *A* and *B* compare clamps which started at equivalent times in the plateau but are of different duration. Panel *A* and *C* compare clamps of

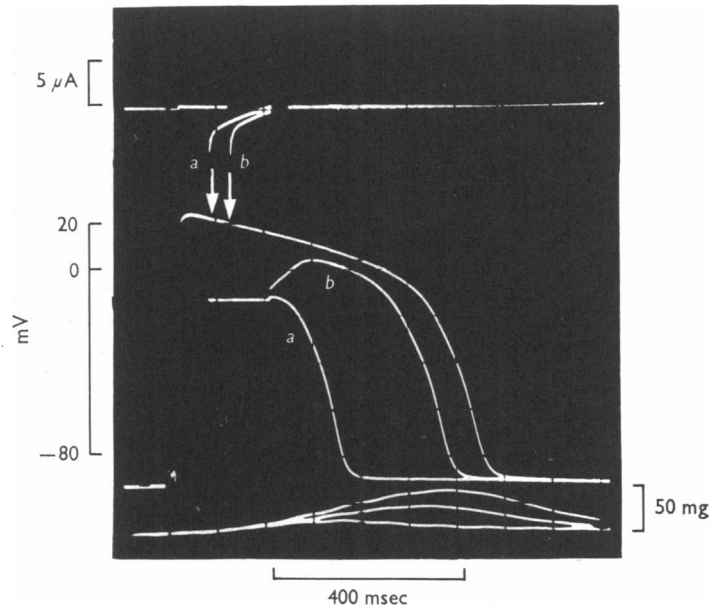

Fig. 5. Superimposed records of an action potential and two voltage clamp pulses of different duration which started 90 and 135 msec after the stimulus (downward arrows). Lower traces, contractile response of the preparation to interrupted action potentials (middle traces). Upper trace, uncompensated voltage clamp current. The shorter pulse, accompanying current trace *b*, resulted in depolarization of the membrane upon release of the clamp. The longer pulse (current trace *a*, which starts earlier) resulted in immediate repolarization.

equal duration but which were initiated at different positions in the plateau. It can be seen that a 50 msec increase in duration of the clamps (panels *A* and *B*) shifts the threshold of repolarization from −33 to −17 mV, whereas a 100 msec change in the clamp position only changed the threshold potential from −33 to −28 mV (panels *A* and *C*). This stronger effect of the clamp duration than the clamp position on the threshold potential was consistently seen throughout the plateau and for various duration clamps. The results of an experiment in which clamp durations were varied from 30 to 150 msec and clamps were started 100–400 msec

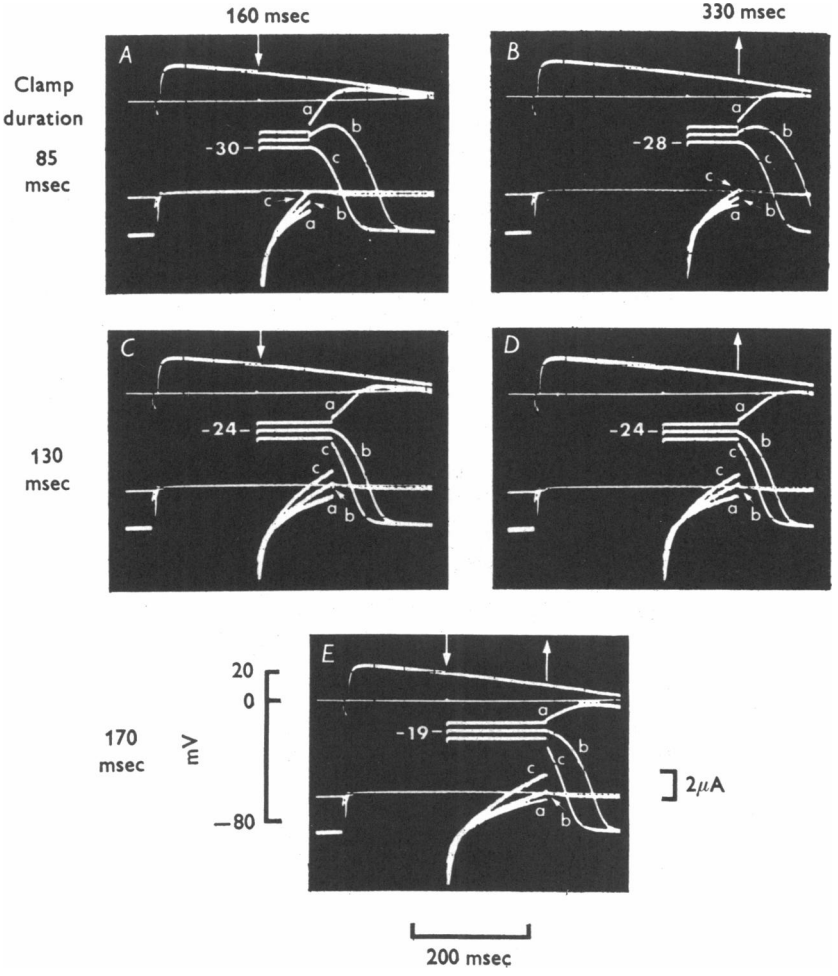

Fig. 6. Comparison of the effect of position and duration of the clamp pulse during the plateau on the apparent 'threshold' of repolarization. Upper traces, membrane potential. Lower traces, uncompensated voltage clamp currents. Records of three test pulses are superimposed in each panel and the threshold value is numerically indicated. The duration of the clamp pulse is varied in different panels: 85 msec in panels *A* and *B*, 130 msec in panels *C* and *D*, and 170 msec in panel *E*. In panels *A*, *C*, and *E*, clamps are initiated 160 msec after the stimulus. In panels *B*, *D*, and *E*, clamps are terminated at 330 msec after the stimulus. In each case, longer duration clamps resulted in a less negative 'threshold' potential whether they started at the same time after the stimulus (panels *A*, *C*, and *E*) or ended at the same time after the stimulus (panels *B*, *D*, and *E*). The clamp duration strongly affects the 'threshold' value.

after the onset of the action potential are shown in Fig. 7*D*. The plotted symbols indicate the threshold potential *vs.* time of termination of each clamp. For instance, the square symbols indicate the threshold potential for 30 msec test pulses (see inset) which started 100, 200, 300, and 400 msec after the stimulus (downward arrows) and are plotted at 130, 230, 330, and 430 msec after the stimulus. The triangular symbols represent the apparent threshold potential for 50 msec clamps (see inset). They are plotted at 150, 250, 350, and 450 msec after the stimulus. The remaining symbols for 75, 100, and 150 msec clamp pulses are similarly plotted vs the time of termination of the clamps. Each series of *connected* symbols started at the equivalent time in the plateau (i.e. the left most curve is for clamps starting 100 msec after the stimulus as indicated by the left most downward arrow). The connected curves show that the threshold potential rose rapidly during the time course of the clamp pulse. Comparison of the rate of shift of the apparent threshold potential for each series of connected symbols with the rate of shift of the threshold for constant duration clamps (e.g. squares or triangles only) shows that the potential of the threshold shifts more rapidly during an anodal clamp than during the time course of the plateau itself. Such results strongly imply that the membrane permeabilities responsible for threshold of repolarization and the initiation of rapid repolarization of the action potential itself are both time and potential-dependent.

Clamp currents during development of regenerative repolarization. Although membrane currents measured in Figs. 4, 5, and 6 have not been corrected for the known artifacts inherent in the single sucrose gap voltage clamp technique such as extracellular leakage current (Morad & Orkand

Fig. 7. Effect of position and duration of the clamp pulse on the apparent threshold of repolarization. Panels *A*, *B*, and *C*, superimposed records of action potentials interrupted by three voltage clamp pulses. The threshold value is indicated numerically. In panels *A* and *B* test pulses of 50 and 100 msec in duration have been applied 200 msec after the stimulus. Prolongation of the clamps by 50 msec (panel *B*) raised the threshold to a value 16 mV less negative. In panels *A* and *C*, the effect of test pulses starting 200 and 300 msec after the stimulus and 50 msec in duration are compared. Delay of initiation of the clamps by 100 msec (panel *C*) raised the threshold to a value 5 mV less negative. In panel *D* the apparent threshold of repolarization for four series of clamps which started 100, 200, 300, and 400 msec after the stimulus (downward arrows) have been plotted. The points plotted are the apparent threshold value versus time of termination of the test clamp. The threshold values for clamp series which started at equivalent plateau times have been connected. Each point on one of the four curves represents the result of various duration clamps as indicated in the inset. The curves represent the rise of threshold value during an anodal clamp pulse. No threshold potential was observed for 10 and 25 msec clamp pulses.

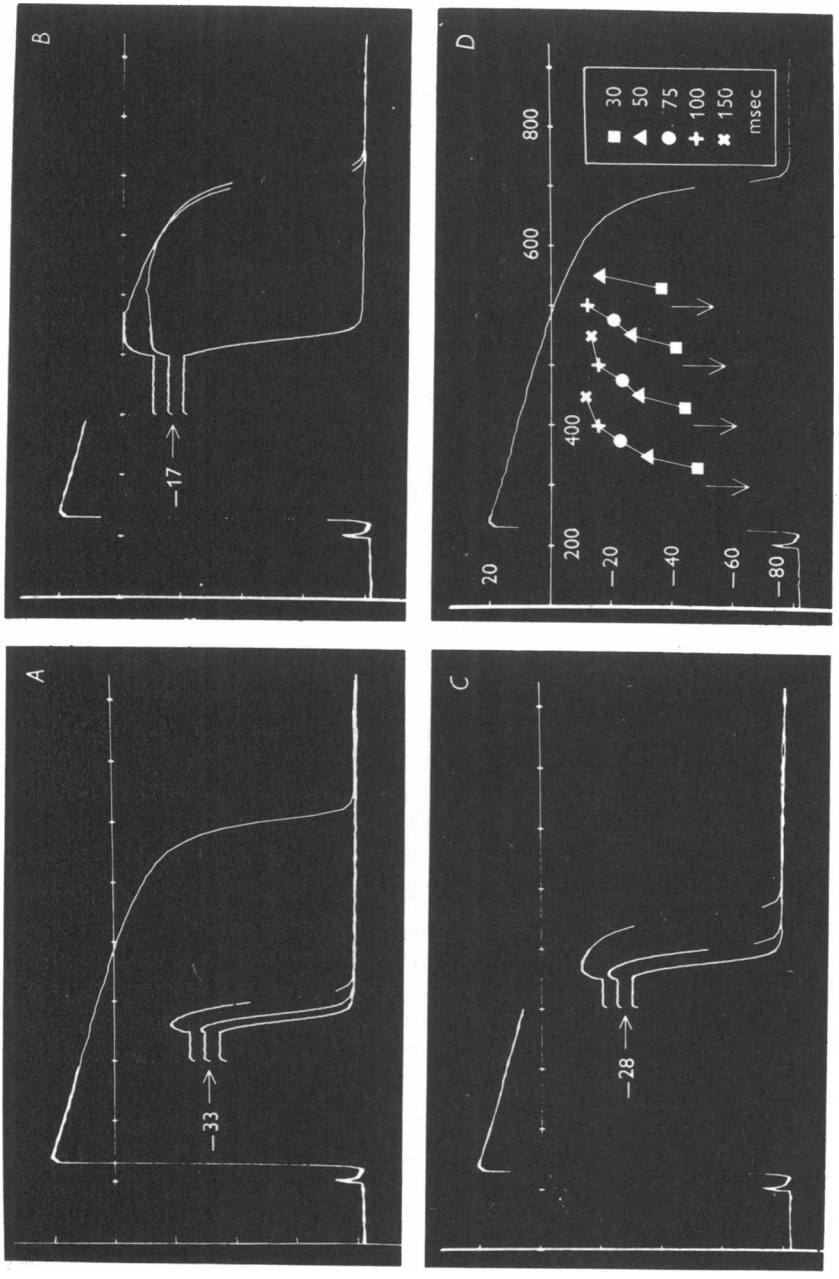

Fig. 7. For legend see facing page.

1971; New & Trautwein, 1972) and extracellular series resistance (Beeler & Reuter, 1970; Tarr & Trank, 1971), certain observations about such recordings (Figs. 4 and 6, lower traces, Fig. 5, upper trace) are pertinent. The transgap currents required to clamp the micro-electrode potential to test levels close to the threshold of repolarization (with the micro-electrode impaled near the centre of the physiological node) have the following characteristics: (1) when the membrane potential is clamped downward from the plateau, the current is initially inward and a time dependent decrease toward zero net current occurs; (2) the current flowing just before termination of the clamp is strictly related to the subsequent membrane potential change upon release of the clamp. That is, if the final clamp current is *inward*, the membrane always *depolarizes* and if the final clamp current is *outward*, the membrane immediately *repolarizes*; (3) the time-dependent decrease of current at more negative clamp potentials: (*a*) is more rapid; (*b*) reaches zero net current earlier in the clamp; and (*c*) is less negative at the end of the clamp. The time dependent decrease of current at less negative test potentials: (*a*) is slower; (*b*) reaches zero net current later in the clamp; and (*c*) is more negative at the end of the clamp; and (4) the threshold for immediate repolarization at each clamp duration is that potential at which the current crosses zero just before the clamp is released. In each panel of Fig. 4, 5, and 6, the current recorded at the critical potential for immediate repolarization is that current trace which *just* reaches or crosses the zero current level at the end of the clamp. Either shorter or less negative clamp steps resulted in an inward final current and caused depolarization upon release of the clamped potential. Clamp steps longer in duration or more negative than the critical potential resulted in outward final clamp current and repolarization.

These results show that the clamp currents recorded with the micro-electrode near the centre of the strip are closely related to the development of the threshold of repolarization. The strict dependence of the rate of post-clamp membrane de- or repolarization to the final clamp current suggests that the same processes underlie the regenerative repolarization and the time dependence of the measured clamp currents even in the absence of any correction for leakage current and extracellular resistance (see also Goldman & Morad, 1977*a*, *b*).

Is the threshold of repolarization instantaneous? Fig. 8 shows clamps of various durations which interrupt the plateau of the action potential in a preparation treated with tetrodotoxin (5×10^{-7} M). Since the upstroke of the action potential was completely suppressed at this concentration of tetrodotoxin, the plateau was initiated by depolarization with a strong transgap current pulse. Interruption of the plateau with very short (10–20 msec) clamp pulses failed to show any threshold potential between

plateau and −60 mV (Fig. 8*A* and *B*). Instead, the membrane depolarized after each clamp and then finally repolarized. Tetrodotoxin was used in the experiment of Fig. 8 to minimize the contribution of the rapid sodium system or possible inhomogeneities due to this current. Similar results were obtained in preparations not treated with tetrodotoxin. Fig. 8*C* shows the appearance of a threshold potential when the plateau was

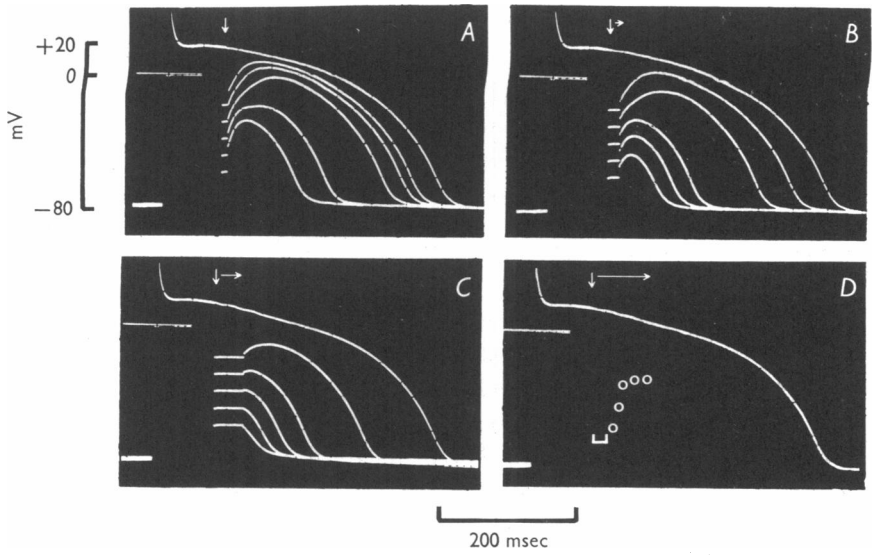

Fig. 8. Apparent 'threshold' potential and short clamp pulses. Panels *A*, *B*, and *C* show the superimposed records of clamp pulses starting 75 msec after the stimulus (downward arrows). Test pulses were 10, 20, and 40 msec long in panels *A*, *B*, and *C* respectively (horizontal arrows). There is no threshold for immediate repolarization with 10 and 20 msec clamp pulses. In panel *D* apparent 'threshold' of repolarization is plotted versus time of termination of the clamps. Bracket marker indicates maximum duration clamps for which there was no threshold. This preparation was bathed in Ringer solution containing tetrodotoxin (5×10^{-7} mole/l.)

interrupted with longer duration clamps. This threshold potential is plotted versus clamp duration (as indicated by the length of the horizontal arrow) in panel *D*. The length of the bracket marker in Fig. 8*D* indicates the duration of short clamps for which there was no threshold potential. As the duration of the clamps was successively prolonged, an apparent threshold potential appeared and became less negative for longer clamps (see also Fig. 7*D*). These findings suggest that there is no unique threshold of repolarization but that the regenerative repolarization phenomenon shown in Figs. 4, 5, 6, 7, and 8 is a time-delayed effect of the test clamp potential.

Approximation to the instantaneous current–voltage relation

The absence of a discrete threshold for immediate repolarization with very short clamps implies that the instantaneous current–voltage relation of the membrane during the plateau has no region of outward current below the plateau potential. The strict dependence of post-clamp de- or repolarization to the current at the end of the clamp suggests an approach for estimation of the membrane current–voltage relation. Since after a clamp, the net membrane current (I_m) is zero, the sum of the ionic (I_i) and capacitive (I_c) currents is zero:

$$I_m = I_i + I_c = I_i + C_m \frac{dV_m}{dt} = 0, \quad I_i = -C_m \frac{dV_m}{dt},$$

where V_m = membrane potential and C_m = membrane capacitance. Therefore, the negative rate of change of membrane potential just after a clamp should be proportional to the ionic membrane current flowing at the end of the clamp. A plot of the negative derivative of membrane potential versus the potential itself ($-dV/dt$ *vs.* V) just after a short clamp should provide a qualitative indication of the membrane current–voltage relation. Such a procedure should also minimize the difficulties inherent in interpreting voltage clamp current records, since at the instant of measurement no net membrane current is flowing.

Fig. 9 shows an experiment in which short (2 msec) clamp pulses interrupted the action potential at two different times (arrows in Fig. 9*A*). Panel *B* shows a series of superimposed records of potentials after termination of clamps which interrupted the plateau. The membrane potential before the clamp pulse was +20 mV. Consider the pulse labelled V_c in Fig. 9*B*. The micro-electrode potential was held at −82 mV (V_c) for 2 msec and then the clamp was terminated. Immediately after the clamp, the measured potential jumped to −27 mV (V_m) and then depolarized more slowly towards the plateau potential. The initial jump in the micro-electrode potential upon termination of the clamp is due to the voltage drop across the extracellular series resistance which has been observed in myocardial preparations (Goldman & Morad, 1977*a*; Beeler & Reuter, 1970; Tarr & Trank, 1971). When the voltage clamp is turned off and no net membrane current flows, the voltage drop across the extracellular series resistance becomes zero. Therefore, the potential labelled V_m in Fig. 9*B* is the true transmembrane potential at the end of the clamp pulse V_c. The slower depolarization after the jump represents charging of the membrane capacitance by ionic current. This initial rate of change of membrane potential versus the true transmembrane potential (V_m) is plotted in Fig. 10, curve *A*, for a series of clamp potentials. Fig. 9*C* shows

another series of clamps which were applied during the final rapid phase of repolarization and the $-dV/dt$ *vs.* V data are plotted in Fig. 10, curve *D*.

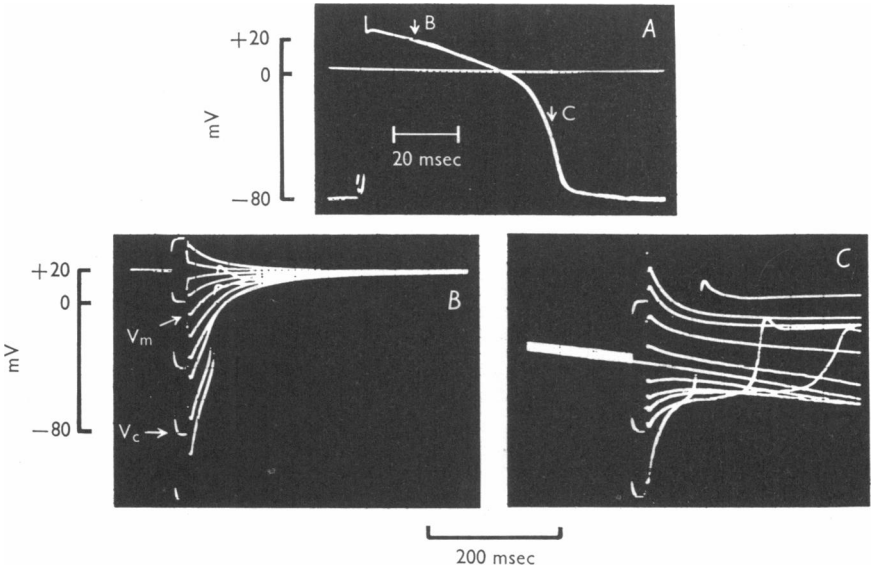

Fig. 9. Short (2 msec) clamp pulses applied during the plateau and during rapid repolarization. In panel *A* downward arrows (*B* and *C*) during the action potential indicate the time at which a series of 2 msec clamp pulses were applied. In panel *B* the superimposed records of 10 clamp pulses applied during the plateau are shown. The command potential (V_c) is indicated for one of the test pulses. The membrane potential at the end of the clamp pulse is marked as V_m. The jump of potential at clamp termination from V_c to V_m is due to extracellular series resistance (Goldman & Morad, 1977*a*). In panel *C* a series of 2 msec clamp pulses are applied during rapid repolarization. The delayed rapid depolarizations for the lowest two pulses in panel *B* and lowest three pulses in panel *C* are probably Na spikes.

For the most negative clamps in Fig. 9*B* and *C*, a second delayed and rapid depolarization occurred after release of the clamp. These rapid depolarizations could be blocked by addition of tetrodotoxin (note absence of such fast delayed depolarization in the experiment of Fig. 8). If the membrane was clamped to potentials less negative than -40 mV, the delayed depolarization did not occur. These results suggest that the delayed depolarizations are due to activation of the rapid Na^+ transport system. In any case, they do not influence the results at potentials less negative than -40 mV.

The $-dV/dt$ *vs.* V data obtained from a series of clamps which interrupted the action potential at four different times are plotted in Fig. 10 (note arrows on the inset action potential). The $-dV/dt$ *vs.* V curves are

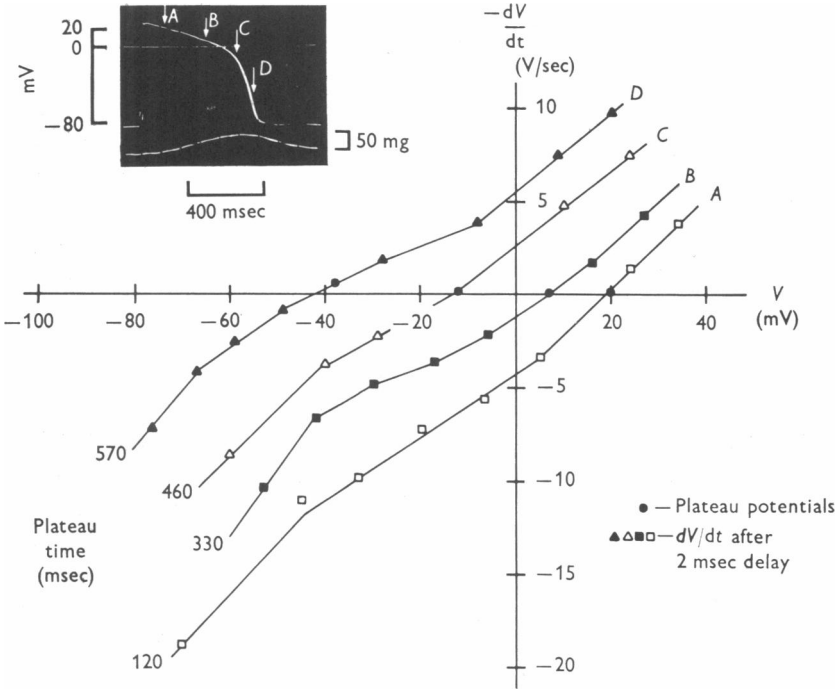

Fig. 10. Pseudo-instantaneous current–voltage relations during the plateau and the repolarization phase of the cardiac action potential. Experimental procedure shown in Fig. 9. Short (2 msec) test clamp pulses are applied at various times during the action potential indicated by downward arrows in the inset. Membrane potential 2 msec after termination of the clamp pulse is plotted vs the negative derivative of membrane potential. The 'pseudo-*I–V*' relations are approximately linear and shift slowly leftward during the plateau. Filled circles represent the membrane potential and repolarization rate of action potential measured with no applied clamp. The membrane potential seems to follow within 1–2 mV of the intersection of the '*I–V*' relation with the abscissa.

pseudo-instantaneous I–V relations measured about 4 msec after a rapid change of membrane potential. The pseudo-I–V curves show no region of negative conductance or outward current below the plateau level and seem to shift very slowly leftward as the plateau progresses. The plateau potential and repolarization rate at the clamp initiation time have been plotted for each curve as indicated by a filled circle. The action potential

follows the intercept on the abscissa of the $-dV/dt$ *vs.* V relation very closely (within 1–2 mV) during the plateau and only deviates from the intercept by about 4 mV during rapid repolarization (curve *D*). To the extent that these curves may be compared with the membrane ionic currents, these results predict that the instantaneous current–voltage relations of the membrane during the plateau have no negative conductance region (see Goldman & Morad, 1977*b* for further discussion of the characteristics of I–V relations in the frog ventricular myocardium).

Approximation of membrane conductance. The slope of a linear instantaneous current–voltage relation is the ionic conductance of the membrane. The conductance of the pseudo-instantaneous I–V relation of Fig. 10 seems to decrease very slightly as the membrane repolarizes during the action potential. That this slope is in fact related to the membrane conductance and not simply an artifact of the cable properties of the muscle is shown by the observation that the measured 'conductance' is markedly higher at rest than during the plateau of the action potential. Fig. 11 shows recordings of a 2 msec clamp pulse applied during the plateau and rest in a preparation treated with tetrodotoxin. In panels 2 and 3, traces marked *A* and *B* are records of clamp pulses positive and negative to the plateau respectively and trace *C* is a hyperpolarizing pulse from rest. The potential labelled V_c (panel 3) is the command potential for trace *B*. As in Fig. 9, upon termination of the 2 msec clamp, the micro-electrode potential jumped to the level labelled V_m due to the extracellular resistance. A slower depolarization then occurred due to flow of inward ionic current through the membrane. The $-dV/dt$ of each pulse has been plotted *vs.* V in panel 1 of Fig. 11. As described above, the $-dV/dt$ *vs.* V curve measured about 2 msec after a 2 msec clamp pulse represents a pseudo-instantaneous current–voltage relation of the membrane at the instant of initiation of the clamp. The slope of the $-dV/dt$ *vs.* V curve is markedly higher at rest than during the plateau which agrees with the results of direct measurement of the conductance (Weidmann, 1951; Goldman & Morad, 1977*a*, *b*).

A quantitative measure of the membrane conductance can be obtained from the time constant of the potential traces in experiments such as that shown in Fig. 11. The average time constant (τ_m) of the membrane measured as the decay of the potential trace after a 2 msec current pulse was 10·9 msec ($\pm$ 3·8 S.D., $n = 5$) during the plateau and 2·1 msec ($\pm$ 1·0 S.D., $n = 5$) at rest. If the membrane capacitance (C_m) is assumed to be 1 μF/cm^2 and is assumed to remain constant during excitation (Cole & Curtis, 1939), then the corresponding membrane conductances are $g_m = C_m/\tau_m = 92$ μmhos/cm^2 during the plateau of the action potential and 322 μmhos/cm^2 at rest.

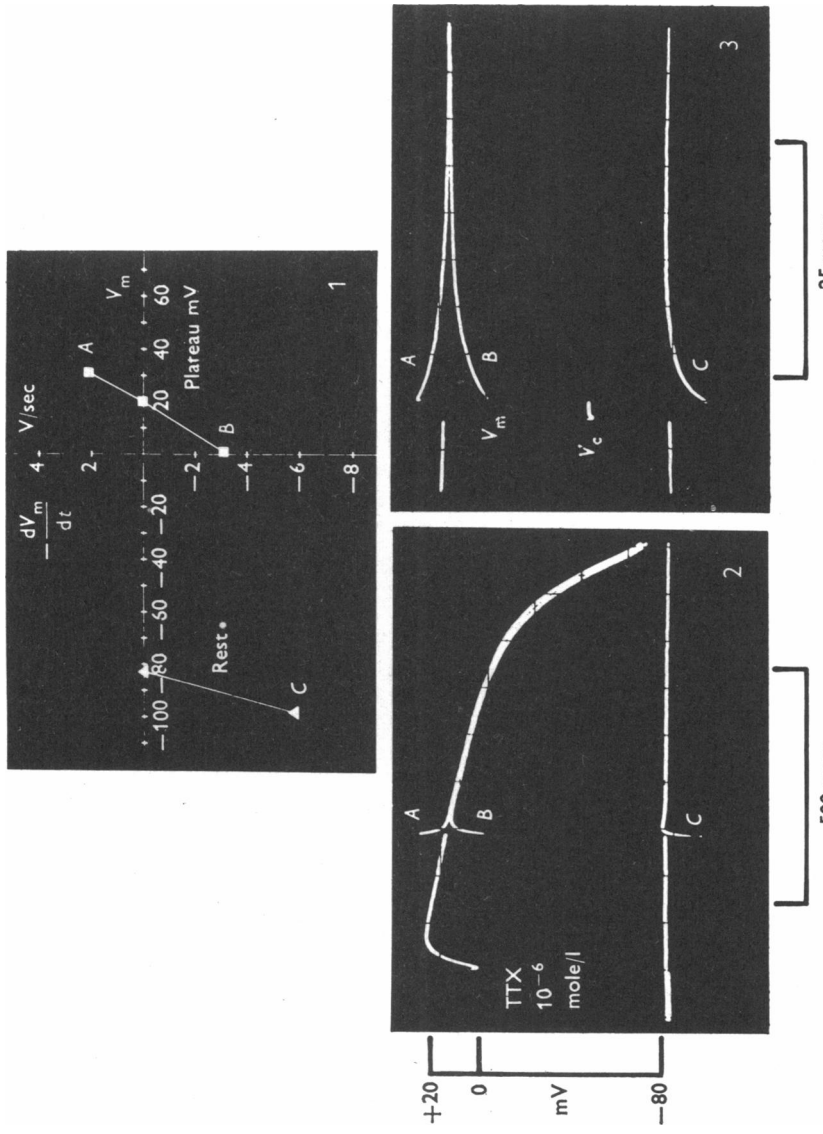

Fig. 11. For legend see facing page.

Validity of the measurement of time and potential dependent repolarization

Break depolarization. The results shown in Figs. 5, 6, 7, and 8 have an increased tendency to repolarize for longer duration clamps. However, the opposite results were observed in some preparations for specific test clamps.

In Fig. 12, a normal action potential has been superimposed upon two subsequent action potentials which were interrupted during the plateau by anodal clamps. The two clamps started at the equivalent plateau and were held at the same potential for different durations as indicated by the arrows. In this experiment, the shorter duration clamp results in immediate repolarization, whereas the membrane depolarized after the longer clamp. Such preparations could be distinguished by four other characteristics: (1) the depolarization generally occurred with clamp potentials more negative than the threshold for immediate repolarization and usually below -40 mV; (2) the action potential generated by 'break depolarization' often rose above the plateau potential and repolarized later than the normal action potential recorded in Ringer solution (compare Figs. 5 and 12); (3) a delayed inward-going 'bump' invariably appeared on the current wave form (Fig. 12); and (4) both the inward current 'bump' and the 'break depolarization' were eliminated by addition of tetrodotoxin (10^{-6} M) to the bathing medium. The addition of tetrodotoxin otherwise had little or no effect on duration of the plateau or the threshold phenomenon (see Fig. 8). These results suggest that depolarization after 100 msec

---

Fig. 11. Pseudo-instantaneous 'current–voltage' relations at rest and during the plateau. Short (2 msec) voltage clamp pulses were applied to the membrane during the plateau (traces *A* and *B* in panels 2 and 3) and at rest (trace *C* in panels 2 and 3). A slow time-base recording is shown in panel 2 to indicate the time in the plateau at which the voltage clamps were initiated (traces *A* and *B*). Panel 3 is a faster time-base recording. The upper left trace is the plateau potential. 280 msec after the stimulus the plateau was interrupted by clamping the membrane to -44 mV (labelled V_c) for 2 msec. Immediately after release of the voltage clamp, the intracellular potential jumped to 0 mV (labelled V_m) due to the extracellular series resistance (Goldman & Morad, 1977*a*) and then more slowly charged toward the plateau level (trace *B*). On a subsequent sweep a depolarizing clamp pulse was applied from the plateau to $+78$ mV (off-scale in the Figure). The response of the membrane after the release of $+78$ mV pulse is shown as trace *A* in panels 2 and 3. A 2 msec clamp pulse to -142 mV was also applied from the resting state (traces *C* in panels 2 and 3). Panel 1 abscissa: membrane potential 2 msec after termination of test clamps. Ordinate: negative derivative of membrane potential 2 msec after termination of the test clamps. The slope of each curve is proportional to membrane conductance which is higher at rest than during the plateau. TTX, tetrodotoxin.

clamps from the plateau of a normal Ringer action potential to below −40 mV were a result of activation of the rapid tetrodotoxin sensitive Na transport system. The wide variation from preparation to preparation of the 'break depolarization' suggests that inhomogeneous distribution of current or potential during voltage clamps in some strips may be respon-

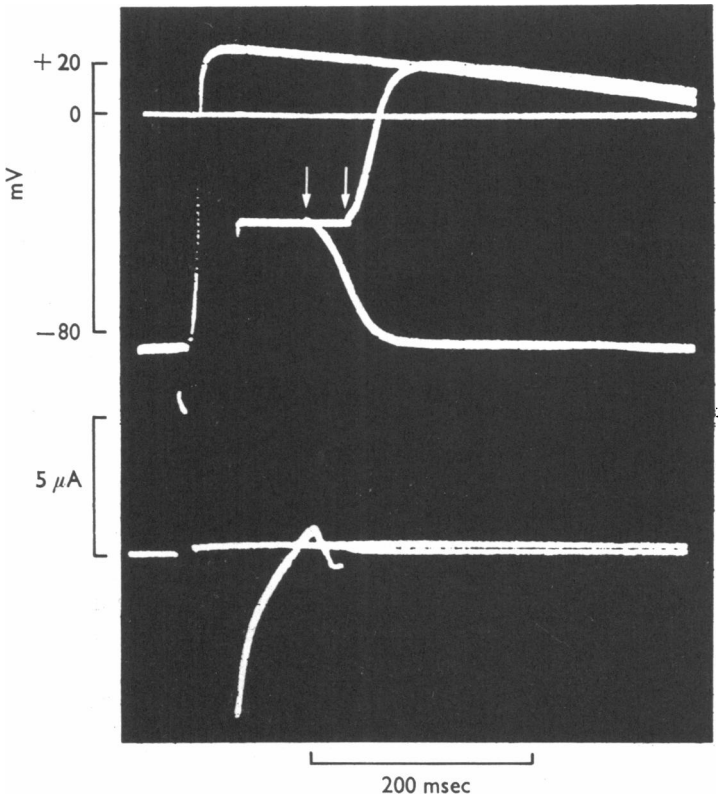

Fig. 12. 'Break depolarization' after the release of clamped potential. Superimposed voltage clamp pulses starting 45 msec after the stimulus and ending 60 and 100 msec later (downward arrows). The longer clamp resulted in 'break' depolarization. Lower traces show the uncompensated voltage clamp currents accompanying the clamp steps. The inward-going 'bump' is followed by the break depolarization.

sible for its appearance. Since tetrodotoxin blocks this effect without significantly altering the plateau or the regenerative repolarization, 'break depolarization' is not related to the ionic events of normal repolarization. Further, the insensitivity of the threshold of repolarization to application of tetrodotoxin indicates that the threshold of repolarization is independent of activation or inactivation of the rapid Na system.

Longitudinal potential distribution in the ventricular strip. Use of the micro-electrode in the feed-back loop of the single sucrose gap voltage clamp technique allows accurate measurement of intracellular potential for long experimental periods. However, a micro-electrode samples the potential of only one cell. It is conceivable that the potentials of other cells, away from the micro-electrode tip, may vary substantially. It might be argued, therefore, that the time dependent repolarization processes are not inherent properties of the individual cell membranes, but result from the distribution of potentials in the strip which slowly approach some equilibrium condition during the clamp. It is conceivable that this possibility could also account for the time dependence of the membrane currents obtained during the clamp steps.

To check for existence of potential variation in the strip, the transgap and intracellular potentials were simultaneously monitored just after termination of the clamp steps. As discussed in the theoretical section, eqn. (1.16) and the Appendix, the transgap potential is an attenuated version of the average intracellular potential at the Ringer-sucrose interface when no current is applied across the sucrose gap. In Fig. 13, the potential of the KCl pool with respect to the Ringer pool (the transgap potential) was recorded in addition to the intracellular potential measured via a micro-electrode. In panel *A*, the two recordings are nearly equal at the beginning of the action potential. When the plateau is interrupted by an anodal voltage clamp step to a test potential less negative than the effective threshold, the final clamp current (bottom trace, panel *A*) is inward and the membrane (V_I) depolarizes upon release of the clamp. The transgap potential (V_G) is off-scale during the clamp pulse because the clamp current is applied at the KCl bath electrode. However, upon termination of the voltage clamp, the transgap potential rapidly returns to within 10 mV of the intracellular potential (Fig. 13*A*). Therefore, the transgap potential also depolarizes and finally follows a repolarization time course similar to that recorded with the micro-electrode.

The difference between the transgap and the intracellular potential in Fig. 13*A* just after termination of the clamp is that V_G is more negative than V_I. This difference is expected from the cable analysis of the theoretical section (Fig. 3*C*) for the case of inward current. A longitudinal internal potential gradient should theoretically exist from the micro-electrode at the centre of the node to the Ringer–sucrose interface. Both the experimentally determined and theoretically predicted longitudinal internal potential gradients in the physiological node are from the micro-electrode towards the sucrose gap during application of inward current (Figs. 3*C* and 13*A*).

It is reasonable to ask whether this potential gradient could be

responsible for the depolarization of the membrane potential observed after release of the clamp in Fig. 13*A*. This might occur if a group of cells were at a potential positive to the impaled cell and were thus electrotonically depolarizing it. But the cells in the ventricular strip between the micro-electrode and the Ringer-sucrose interface (and for that matter, throughout the entire sucrose gap; see Fig. 3*C*) are at potentials negative to the impaled cell. Therefore, the existing longitudinal potential gradient be-

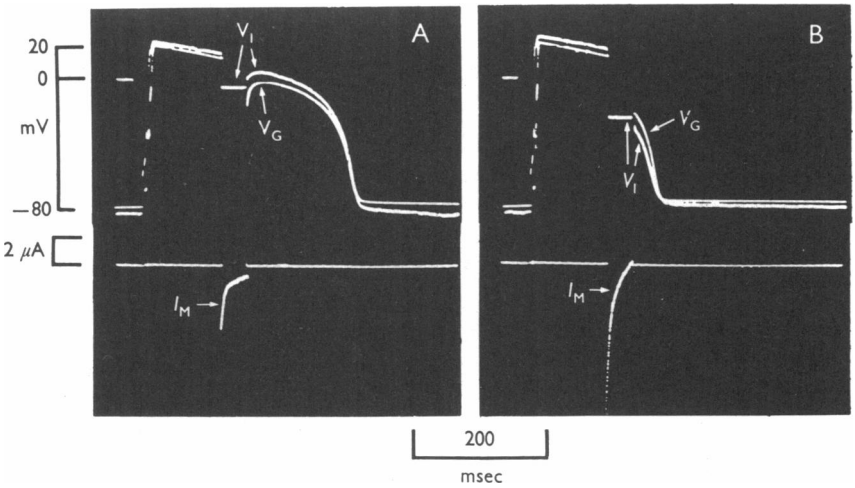

Fig. 13. Superimposed intracellular (V_I) and transgap (V_G) measurements of membrane potential during a threshold of repolarization experiment. The lower traces show uncompensated voltage clamp current (I_M). In panel *A*, the test voltage clamp step is more positive than the apparent 'threshold' potential. The final clamp current is inward (plotted downward) and the membrane depolarizes upon release. Transgap potential (V_G) is more negative than the intracellular potential (V_I) after the clamp. In panel *B*, the test voltage clamp is more negative than the apparent threshold potential. The final clamp current is outward (plotted upward) and the membrane (V_I) immediately repolarizes upon release. The transgap potential (V_G) is more positive than the intracellular potential (V_I) after release of the clamp. These potential gradients are predicted by the cable model shown in Fig. 2.

tween the micro-electrode and the KCl bath is in the wrong direction to be the cause of the depolarization observed after the release of the clamp and if anything would tend to suppress the depolarization.

Experimental determination of the longitudinal gradient for the opposite case (i.e. outward current) is shown in Fig. 13*B*. The plateau is interrupted by a clamp step to below the effective threshold potential. The final clamp current is outward and, as expected, the membrane

immediately repolarizes. V_G, in this case, is positive with respect to V_I just after the clamp. This finding is consistent with the analysis of the idealized cable model for the case of the outward current (Fig. 3*B*) which predicts a potential gradient from the sucrose gap toward the micro-electrode position. Thus, the cells between the micro-electrode and the sucrose gap are positive with respect to the impaled cell and would tend to depolarize it electrotonically. The immediate repolarization seen in Fig. 13*B*, therefore, cannot be due to the longitudinal potential gradient between the micro-electrode and the sucrose gap since the measured gradient is in the wrong direction to repolarize the membrane. Thus, voltage dependent repolarization after clamp steps cannot result from the longitudinal potential gradients between the micro-electrode (at the centre of the strip) and the sucrose-Ringer interface.

Since the threshold for immediate repolarization was also seen to depend on the clamp duration (Figs. 5, 6, 7, and 8), it was of interest to determine the possible effect of the potential gradient on time dependent repolarization. Fig. 14 shows transgap and intracellular recordings of action potentials interrupted during the plateau by clamps of different durations. In panels *A* and *B*, duration of the pulses were short enough so that the membrane depolarized upon release of the clamp. In both cases, the final clamp current is inward and V_G is negative to V_I. The potential gradient is in the micro-electrode-to-sucrose direction so that the cells between the micro-electrode and sucrose gap would tend to electrotonically suppress rather than cause the depolarizations after the clamps (Fig. 3*C*). In Fig. 14*C*, the clamp is long enough to result in outward final membrane current and repolarization. In this case V_G is positive to the intracellular potential sampled by the micro-electrode at the centre of the strip. The potential gradient, however, is in the direction which would tend to depolarize rather than immediately repolarize the membrane. Thus, the experimentally measured longitudinal potential gradient for time and potential-dependent repolarization are consistent with the predictions of the idealized cable model and cannot be responsible for the threshold phenomenon.

The longitudinal potential gradient considered above and shown not to contribute to the threshold of repolarization was determined only for the region of the preparation between the micro-electrode and the sucrose gap. According to the theoretical analysis (Fig. 3), the longitudinal gradient in the other half of the physiological node, i.e. between the micro-electrode and the free end of the muscle, should be in such a direction so as to contribute to the membrane potential changes observed upon release of the clamps. For instance, in the case of applied net inward current the cells at the end of the muscle should be at a less negative potential than the impaled cell (Fig. 3*C*). Thus, upon the release of a clamp they could

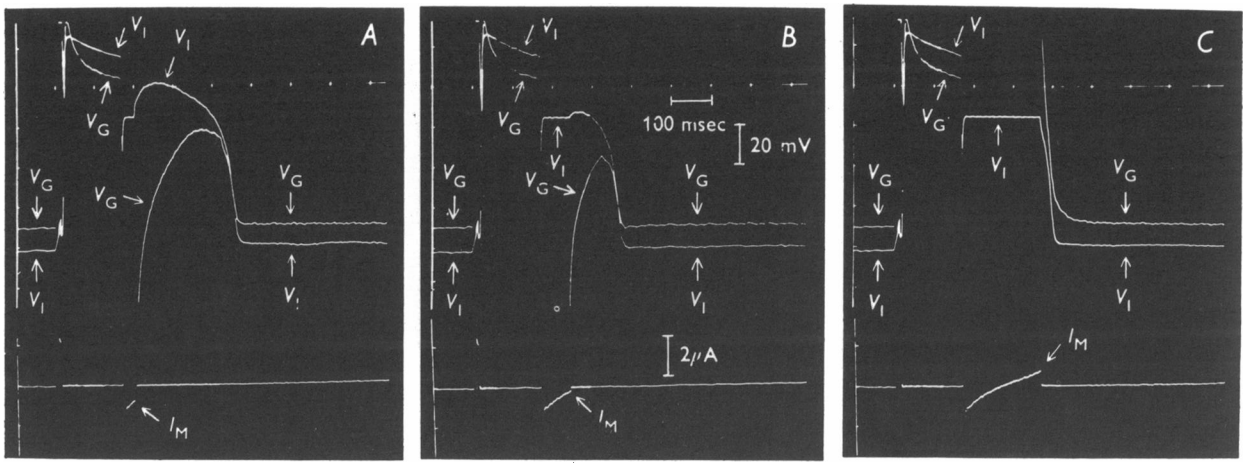

Fig. 14. Superimposed intracellular (V_I) and transgap (V_G) measurements of membrane potential during the development of a repolarizing condition. The lower traces show the time course of the uncompensated voltage clamp current (I_M). In panels *A* and *B* the action potential is interrupted with 30 and 75 msec clamp pulses respectively. The final clamp current is inward (plotted downward) and the membrane (V_I) depolarizes upon release. Transgap potential (V_G) is more negative than the intracellular potential (V_I) after the release of the clamp. In panel *C*, a 200 msec voltage clamp step produces an outward final membrane current (plotted upward) and thus causes immediate repolarization upon release of the clamp. In this case the transgap potential (V_G) is more positive than the intracellular potential (V_I) after release of the clamp. These potential gradients are predicted by the cable model of Fig. 2.

electrotonically depolarize the cell in the centre of the strip in which the micro-electrode is placed. To test the extent of this contribution to the threshold of repolarization, the two types of experiments were performed: (1) the contributing region of the strip was minimized by placing the feedback micro-electrode at the free end of the physiological node (see inset, Fig. 15*A*); (2) the contributing region was maximized by impaling a cell near the Ringer-sucrose interface (see inset, Fig. 15*C*).

Fig. 15*A* shows the time course of potential change after the release of a short anodal (inward current) clamp pulse when the micro-electrode is placed at the free end of the muscle. Under this condition, the bulk of the cells of the preparation are at more negative potentials than the impaled cell (Fig. 3*C*). The electrotonic effect of the longitudinal gradient is, therefore, to maximally repolarize the impaled cell upon release of the clamp. In fact, in Fig. 15*A*, termination of the clamp resulted in a rapid transient repolarization due to the electrotonic equilibration of the longitudinal potential gradient. Thereafter, the membrane depolarized toward the plateau potential and then finally repolarized. There is no longitudinal region of the strip which could be responsible for this depolarization on the grounds of the potential gradient. On the contrary, cable properties of the muscle would, if anything, diminish the ability of the membrane to show depolarization upon release of the clamp.

In Fig. 15*B*, a depolarizing clamp (outward current) has been applied with the micro-electrode still at the end of the muscle. Consistent with the prediction of the cable model (Fig. 3*B*), the transient electrotonic equilibration after the clamp further depolarizes the impaled cell. Thereafter, the membrane repolarizes to resting level. Comparison of panels *A* and *B* shows that responses to depolarizing the hyperpolarizing currents are qualitatively similar but opposite in direction. This indicates that the processes involved are relatively linear cable properties rather than irregular spacial inhomogeneities or actively conducted 'break' depolarizations such as that shown in Fig. 12.

Fig. 15*C* and *D* are recordings from the same strip in which the micro-electrode was moved very close (75 μm) to the sucrose gap, thus maximizing the region which could electrotonically contribute to an *apparent* threshold phenomenon. Depolarization after the inward current pulse (panel *C*) and repolarization after the outward pulse (panel *D*) are very rapid after release of the clamps. The direction as well as rate of these potential changes can be explained if the intrinsic membrane properties and the longitudinal cable properties were both contributing to the time course of the potential change.

The agreement of the physiological results with predictions of the cable analysis implies that the time course of development of the threshold of

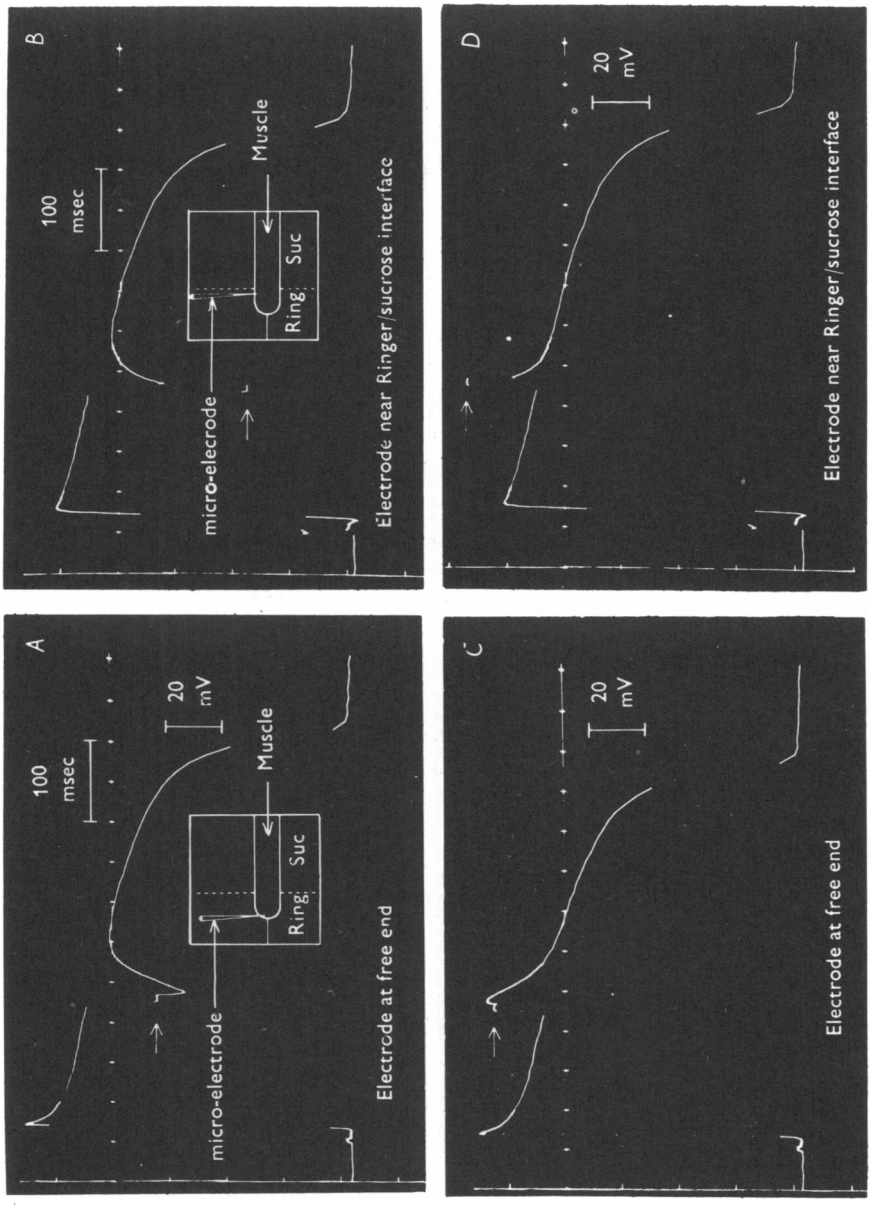

Fig. 15. For legend see facing page.

repolarization phenomenon is not due to longitudinal potential gradients in the ventricular strip. This analysis and the presence of the threshold phenomenon in preparations treated with tetrodotoxin provide strong evidence that the time and potential dependence of the threshold of repolarization are inherent membrane properties rather than artifacts produced by spacial inhomogeneity or cable properties of the ventricular strip.

DISCUSSION

The main observation of this report is that there is no distinct threshold for immediate repolarization of the frog ventricular action potential when the plateau is interrupted by brief (< 20 msec) anodal voltage clamp pulses. However, when the plateau was interrupted by anodal clamp pulses longer than 30–50 msec a critical potential was observed below which the membrane immediately repolarized. This threshold potential slowly became less negative as the plateau progressed and intersected the action potential near the beginning of the rapid repolarization phase. Analysis of longitudinal potential distributions in the ventricular strips showed that the time and potential dependence of the threshold phenomenon are not due to *longitudinal* potential gradients. For instance, when the applied current is inward at the end of a clamp, the membrane depolarizes after the release of the clamp. The measured potential gradient in the muscle during such a clamp step agrees qualitatively with predictions of an idealized cable model (Fig. 3) and indicates that most cells of the preparation (from micro-electrode to KCl bath) are at more negative potentials than the one cell which is measured by the micro-electrode. The electrotonic effect of the potential gradient is in such a direction as to repolarize the impaled cell, but the experimental observation is that the membrane depolarizes upon the release of the clamp. Therefore, the depolarization cannot be due to a longitudinal potential gradient in the muscle.

It is significant to note that the analysis presented does not depend on the specific properties of the simple cable model discussed in the theoretical

---

Fig. 15. Voltage clamp pulses applied with the controlling intracellular electrode placed in different positions in the ventricular strip. In panels *A* and *B* the electrode is placed at the free end of the preparation (see inset, panel *A*). The anodal clamp pulse resulted in a transient repolarization, depolarization, and then final repolarization (panel *A*). A cathodal clamp pulse resulted in a transient depolarization before the final repolarization (panel *B*). In panels *C* and *D* the electrode is placed near the Ringer sucrose interface (see inset, panel *C*). The anodal (panel *C*) and cathodal (panel *D*) clamp pulses result in a rapid return to near plateau level before the final repolarization.

section (Figs. 2 and 3). This model is undoubtedly an oversimplification of the geometrical properties of the ventricular strip in a sucrose gap because active membrane properties, radial potential gradients, and mixing at the Ringer-sucrose interface have been ignored. However, any model in which the cells are assumed to be electrotonically connected will result in the same direction of longitudinal potential gradient during the application of inward current. Net applied current entering cells near the free end of the muscle must flow intracellularly toward the sucrose gap (Fig. 3*C*). The intracellular resistance to this longitudinal current flow must cause the development of a potential gradient in the muscle in the Ringer-to-sucrose direction. Therefore, the measured longitudinal gradients (Figs. 13, 14 and 15) are not specifically related to the simple cable model of Fig. 2, but are, in fact, a direct consequence of electrotonic current spread in the muscle.

Radial potential gradients. Differences between the membrane potential of the surface and the more central fibres were not measured systematically in these experiments. However, reasoning analogous to the case of longitudinal potential gradients can be applied to analyse the possible effects of radial potential gradients on the development of the threshold of repolarization. For instance, outward current flows from centrally located cells towards peripheral cells and exits the muscle from the periphery (Fig. 3). The intracellular resistance to this *radial component* of electrotonic current will cause a potential gradient directed from the core toward the periphery of the muscle bundle. Therefore, the cells in the core region will be at more positive potentials than the peripheral cells where the controlling μ-electrode is placed. After the clamp, the core cells would tend to electrotonically depolarize the impaled cell. Thus, the measured repolarization is not due to radial or longitudinal potential gradients, but must be primarily a true property of the membrane itself.

Conversely, shorter duration or more positive test clamp pulses result in inward final clamp current and membrane depolarization. Radial current flowing from the periphery toward the core of the muscle (Fig. 3*B*) should cause a potential gradient to develop with the centrally located cells at more negative potentials than the impaled peripheral cells. The radial potential gradient should tend to repolarize the impaled cell. Therefore, the observed membrane *depolarization* is not due to the existence of a longitudinal or radial potential gradient.

The theoretical conditions required to demonstrate a threshold of repolarization in various geometrical arrangements have been calculated previously (Noble, 1962*b*; Noble & Hall, 1963). It was shown that with point polarization of a simulated sheet or cable structure, a threshold potential for regenerative repolarization may be difficult to demonstrate

even if the membrane current–voltage relation were N-shaped. However, these computations do not apply to the experimental findings of this report since the current was not applied at a point and the measuring electrode was placed away from the source of polarizing current.

The effects of potential gradients in the muscle during a voltage clamp step were exaggerated in some experiments by placing the controlling micro-electrode in a peripheral cell near the longitudinal end of the muscle in the Ringer pool (Fig. 15*A* and *B*). During inward current flow, the bulk of other cells in the longitudinal and radial directions are at more negative potentials. After termination of the clamp pulse, a rapid and transient repolarization of the impaled cell indicates the electrotonic redistribution of potential in the muscle. However, this effect is then followed by membrane depolarization which cannot be due to longitudinal or radial inhomogeneities of potential distribution but must be a property of the myocardial cell membrane.

Implication of the threshold of repolarization. A critical potential for regenerative repolarization has been observed in a number of other preparations (dog ventricle: Cranefield & Hoffman, 1958; sheep Purkinje fibres: Weidmann, 1951; Vassalle, 1966; frog nerve: Tasaki, 1956), and has been used to infer properties of the membrane current–voltage relation (Noble & Tsien, 1972). It has been argued that the depolarization which occurs above the critical potential must be caused by the flow of inward ionic current and the immediate repolarization which occurs below the threshold indicates flow of outward current. Thus, the appearance of a threshold phenomenon implies that the membrane I–V relation must have a region of inward current below the plateau and at more negative potentials a region of outward current. That is, the I–V relation is N-shaped (Noble & Tsien, 1972).

The observation reported in this paper that the membrane always depolarized after very short anodal clamp pulses (Fig. 8*A*), even in strips treated with tetrodotoxin, implies that the ionic current flowing at the end of these short clamps and during the subsequent depolarization is inwardly directed. The absence of a discrete threshold between plateau and resting potentials for these short clamps suggests that the 'instantaneous' current–voltage relation of the membrane has no region of outward current below the plateau potential. An estimate of the shape of the instantaneous I–V relation during the plateau indicated that there is no region of outward current or negative slope conductance below the plateau potentials. In fact, the pseudo-instantaneous-I–V relations (Fig. 10) are fairly linear and seem to shift slowly upward during the time course of repolarization.

Is there a unique threshold of repolarization? These experiments suggest

that instantaneously, or for short (< 20 msec) test pulses, no threshold of repolarization exists in frog ventricular muscle. However, a threshold for immediate repolarization is observed after longer test pulses as shown in this report and in other myocardial preparations. Therefore, the threshold phenomenon and the N-shaped I–V relations result from time-dependent permeability changes which occur rapidly during the application of the anodal test pulse. This situation is qualitatively similar to the nerve membrane in which the threshold for excitation is a time delayed effect of membrane potential (Hodgkin & Huxley, 1952). However, the development of threshold for repolarization in the heart muscle is much slower.

The absence of a threshold for the short clamp steps has fundamental implications for the nature of the repolarization process. The shift from a depolarizing condition to a repolarizing state during a voltage clamp step implies that a *time dependent* change of ionic permeabilities rather than an instantaneous negative conductance causes the repolarization. This permeability change is also the mechanism of rapid repolarization of the action potential itself because the threshold potential intersects the action potential near the beginning of the rapid repolarization.

A computer simulation of currents recorded during clamp pulses used to test for the threshold of repolarization predicts the shape of the *uninterrupted* action potential (Y. Goldman and M. Morad, unpublished observation). Therefore, the time and voltage dependent currents which cause the threshold of repolarization are also responsible for the rapid repolarization of the action potential itself.

Ionic accumulations and repolarization. Extracellular K^+ accumulation or intracellular Ca^{2+} accumulation might be considered as possible mechanisms for triggering the final phase of repolarization of the cardiac action potential. The threshold of repolarization experiments presented in this report suggest that ionic accumulations are not primary triggers of rapid repolarization.

Significant extracellular K^+ accumulation was measured with K^+-sensitive micro-electrodes during the time course of a frog ventricular action potential (Kline & Morad, 1975). Since elevation of $[K]_o$ increases the repolarization rate of the action potential (Weidmann, 1956) and the outward K^+ currents (Hall, Hutter & Noble, 1963), it might be suggested that local K^+ accumulations cause the final repolarization phase of the action potential. However, the accumulation of K^+ with a 2–8 sec clamp pulse is significantly smaller at membrane potentials of -30 to -20 mV than at the plateau range (-5 to $+15$ mV) (Cleemann & Morad, 1974) and yet the repolarizing condition develops more rapidly at -20 to -30 mV than during the plateau (Fig. 7). Therefore, the rapid repolarization cannot be due to an *accelerated* rate of K^+ accumulation.

Similarly, intracellular accumulation of Ca^{2+} may be dismissed as the primary trigger of permeability changes which repolarize the membrane. The rate of accumulation of Ca^{2+} is less during an anodal clamp pulse from the plateau than during the plateau itself, since the development of tension is suppressed at more negative potentials (Fig. 5, traces *a* and *b*). Therefore, the regenerative repolarization is not primarily dependent on accumulation of Ca^{2+} or K^+. The experiments reported here suggest that the membrane permeability changes which cause the threshold of repolarization and generate the normal action potential are time and voltage dependent.

In the following two papers a method is described which makes it possible to measure the membrane conductances during the plateau and during the development of threshold of repolarization to determine the ionic nature of these permeability changes.

APPENDIX

An electrical schematic of an idealized cable model of a myocardial strip in the single sucrose gap apparatus is shown in Fig. 2. The model was first provided by Sir Alan Hodgkin and has been discussed by R. Tsien (McGuigan, 1974) in a form modified for the double sucrose gap. The fundamental assumption of the model is that the extracellular resistance of the ventricular tissue in the longitudinal direction is greater in the sucrose region than in the Ringer pool. The form presented here is similar to the model derived by Tsien (McGuigan, 1974) except in the following details: (1) it is derived for a single sucrose gap; (2) longitudinal internal and membrane resistivities are allowed to differ between the Ringer and sucrose regions; (3) membrane equilibrium potentials are not assumed to be zero.

Let a heart muscle strip in an idealized single sucrose gap have the longitudinal cable structure shown in Fig. 2. Let the parameters of the model be as listed in the text. Assume

(*a*) linear and passive longitudinal and membrane resistivities;

(*b*) steady-state current and voltage distributions;

(*c*) no longitudinal current flow from the end of the muscle in the Ringer pool (an open circuit termination);

(*d*) zero extracellular longitudinal resistivity in the Ringer pool;

(*e*) no radial potential gradients in the muscle;

(*f*) negligible mixing of solutions at the Ringer-sucrose interface;

(*g*) length of the sucrose gap considerably greater than the longitudinal space constant in the sucrose region.

Then in Ringer and sucrose compartments,

$$\frac{dV_i}{dx} = r_i i_i, \tag{1.1}$$

$$\frac{dV_o}{dx} = +r_o i_o, \tag{1.2}$$

$$\frac{di_i}{dx} = +i_m, \tag{1.3}$$

$$\frac{di_o}{dx} = -i_m, \tag{1.4}$$

$$i_m = \frac{(V_m - E_m)}{r_m}, \tag{1.5}$$

$$\frac{dV_m}{dx} = \frac{d(V_i - V_o)}{dx} = r_i i_i - r_o i_o, \tag{1.6}$$

$$\frac{d^2V_m}{dx^2} = \frac{r_i + r_o}{r_m}(V_m - E_m) = \frac{V_m - E_m}{\lambda^2},$$

where $$\lambda = \sqrt{\frac{r_m}{r_i + r_o}} = \text{space constant (cm)}.$$

The general solution is

$$V_m = E_m + \alpha e^{+x/\lambda} + \beta e^{-x/\lambda}, \tag{1.7}$$

where V_m and x are the only variables. The boundary conditions which determine α and β for the short segment in the Ringer pool are the negligible extracellular resistance $r_o = 0$ and the open circuit termination at $x = 0$:

$$i_i|_{x=0} = 0.$$

The solution is

$$V_m = E_m + (V_e - E_m)\cosh(x/\lambda), \quad 0 \leqslant x \leqslant 1.$$

Since $V_o = 0$ in the Ringer pool:

$$V_i = V_m = E_m + (V_e - E_m)\cosh(x/\lambda), \quad 0 \leqslant x \leqslant 1. \tag{1.8}$$

The membrane potential at the Ringer-sucrose interface, $x = 1$ is

$$V_l = E_m + (V_e - E_m)\cosh(l/\lambda) = E_m + (V_e - E_m)\cosh L, \tag{1.9}$$

where $$L = l/\lambda, \quad V_i = E_m + (V_l - E_m)\frac{\cosh(x/\lambda)}{\cosh(l/\lambda)}. \tag{1.10}$$

Three boundary conditions determine α and β of eqn. (1.7) in the sucrose region. Boundary condition a is: at $x = \infty$, V_m is finite. Therefore, α of eqn. (1.7) is zero in the sucrose region. Boundary conditions

b and c are that the intracellular and extracellular potentials are continuous across the Ringer-sucrose interface. That is,

$$V_i|_{x=1,\,\text{sucrose}} = V_i|_{x=1,\,\text{Ringer}} = V_1,$$
$$V_o|_{x=1,\,\text{sucrose}} = V_o|_{x=1,\,\text{Ringer}} = 0,$$
$$V_m|_{x=1,\,\text{sucrose}} = V_i - V_o = V_1.$$

Combining with (1.1), with $\alpha = 0$ and noting that E_{ms} and λ_s may not equal E_m and λ,

$$V_1 - E_{ms} = [\beta\, e^{-1/\lambda_s}],$$
$$\beta = [V_1 - E_{ms}]\, e^{1/\lambda_s},$$
$$V_m = E_{ms} + (V_1 - E_{ms})\, e^{-(x-1)/\lambda_s} \quad x \leqslant 1 \leqslant \infty. \tag{1.11}$$

To evaluate V_i and V_o in the sucrose region consider the region at $x = +\infty$ (or $(x-1) \gg \lambda$). In this region,

$$V_m = E_{ms}, \quad x = +\infty.$$

By eqn. (1.6): $$\frac{dV_m}{dx} = 0 = r_{is} i_i - r_{os} i_o, \quad x = \infty.$$

The total applied current (I) is

$$I = i_i + i_o,$$
$$i_o = \frac{r_{is} I}{r_{is} + r_{os}}, \quad x = \infty. \tag{1.12}$$

To calculate i_o at any x integrate 1.4

$$\int_{i_o(x)}^{i_o(\infty)} di_o = -\int_x^\infty i_m\, dx = -\int_x^\infty \frac{(V_m - E_{ms})}{r_{ms}}\, dx.$$

Combine with (1.11)

$$i_o(\infty) - i_o(x) = -\int_x^\infty \frac{(V_1 - E_{ms})}{r_{ms}}\, e^{-(x-1)/\lambda_s}\, dx,$$
$$i_o(\infty) - i_o(x) = -\frac{(V_1 - E_{ms})\lambda_s}{r_{ms}}\, e^{-(x-1)/\lambda_s}.$$

Combine with 1.12

$$i_o = \frac{(V_1 - E_{ms})\lambda_s}{r_{ms}}\, e^{-(x-1)/\lambda_s} + \frac{r_{is} I}{r_{is} + r_o}, \quad 1 \leqslant x \leqslant \infty. \tag{1.13}$$

V_o is evaluated by integrating (1.2)

$$\int_{V_o(1)}^{V_o(x)} dV_o = \int_1^x r_{os} i_o\, dx,$$
$$V_o(x) - V_o(1) = r_o \int_1^x \left[\frac{(V_1 - E_{ms})\lambda_s}{r_{ms}}\, e^{-(x-1)/\lambda_s} + \frac{r_{is} I}{r_{is} + r_{os}}\right] dx.$$

But $V_o(1) = 0$; so

$$V_o(x) = r_{os}\left[-\frac{(V_1-E_{ms})\lambda_s^2}{r_{ms}}e^{-(x-1)\lambda_s}+\frac{(V_1-E_{ms})\lambda_s^2}{r_{ms}}+\frac{r_{is}I(x-1)}{r_{is}-r_{os}}\right].$$

But $\lambda_s^2 = (r_{ms}/(r_{is}+r_{os}))$; so

$$V_o = \frac{(V_1-E_{ms})r_o}{r_{is}+r_{os}}(1-e^{-(x-1)\lambda_s})+r_pI(x-1), \quad 1 \leqslant x \leqslant \infty, \quad (1.14)$$

where

$$r_p = \frac{r_{is}r_{os}}{r_{is}+r_{os}},$$

$$V_i = V_o+V_m = \frac{V_1r_o+E_{ms}r_{is}}{r_{is}+r_{os}}+\frac{(V_1-E_{ms})r_{is}}{r_{is}+r_{os}}e^{-(x-1)\lambda_s}+r_pI(x-l),$$
$$1 \leqslant x \leqslant \infty. \quad (1.15)$$

Eqns. (1.9), (1.4), and (1.15) give the intracellular (V_i) and extracellular (V_o) potentials of the muscle in the Ringer and sucrose regions. These equations are plotted in Fig. 3 for various cases of applied sucrose gap currents.

We acknowledge the technical assistance of Mr J. Sonsino, Mr G. Martin and Ms R. Keris. This work was supported by N. I. H. grants HL 13288, HL 16152, and GM 02046.

REFERENCES

BEELER, G. W., JR. & REUTER, H. (1970). Voltage clamp experiments on ventricular myocardial fibres. *J. Physiol.* **207**, 165–190.

BRADY, A. J. & WOODBURY, J. W. (1960). The sodium-potassium hypothesis as the basis of electrical activity in frog ventricle. *J. Physiol.* **154**, 385–407.

CLEEMANN, L. & MORAD, M. (1974). K^+ accumulation in the extracellular space of frog ventricular muscle during long depolarizing clamps. *Fedn Proc.* **33**, 432.

COLE, K. S. & CURTIS, H. J. (1939). Electric impedance of the squid giant axon during activity. *J. gen. Physiol.* **22**, 649–670.

CRANEFIELD, P. F. & HOFFMAN, B. F. (1958). Propagated repolarization in heart muscle. *J. gen. Physiol.* **41**, 633–649.

DE MELLO, W. C. (1972). The healing-over process in cardiac and other muscle fibers. In *Electrical Phenomena in the Heart*, ed. DEMELLO, W. C., New York: Academic Press.

DUDEL, J., PEPER, K., RÜDEL, R. & TRAUTWEIN, W. (1967). The effect of tetrodotoxin on the membrane current in cardiac muscle (Purkinje fibres). *Pflügers Arch. ges. Physiol.* **295**, 213–226.

GOLDMAN, Y. & MORAD, M. (1973). Mechanism of repolarization of the cardiac action potential plateau. *Fedn Proc.* **32**, 417.

GOLDMAN, Y. & MORAD, M. (1977*a*). Measurement of transmembrane potential and membrane current in cardiac muscle: a new voltage clamp method. *J. Physiol.* **268**, 613–654.

GOLDMAN, Y. & MORAD, M. (1977*b*). (Ionic membrane conductance during the time course of cardiac action potential. *J. Physiol.* **268**, 655–695.

HAGIWARA, S. & NAGAJIMA, S. (1966). Differences in Na and Ca spikes as examined by application of tetrodotoxin, procaine and manganese ions. *J. gen. Physiol.* **49**, 793–806.

HALL, E. A., HUTTER, O. F. & NOBLE, D. (1963). Current–voltage relations of Purkinje fibres in sodium-deficient solutions. *J. Physiol.* **166**, 225–240.

HODGKIN, A. L. & HUXLEY, A. F. (1952). A quantitative description of membrane current and its application to conduction and excitation in nerve. *J. Physiol.* **117**, 500–544.

KLINE, R. & MORAD, M. (1975). K^+ accumulation in frog ventricular muscle. *Fedn Proc.* **34**, 360.

MCGUIGAN, J. A. S. (1974). Some limitations of the double sucrose gap and its use in a study of the slow outward current in mammalian ventricular muscle. *J. Physiol.* **240**, 775–806.

MORAD, M. & ORKAND, R. K. (1971). Excitation-contraction coupling in frog ventricle: evidence from voltage clamp studies. *J. Physiol.* **219**, 167–189.

NEW, W. & TRAUTWEIN, W. (1972). Inward membrane currents in mammalian myocardium. *Pflügers Arch. ges. Physiol.* **334**, 1–23.

NOBLE, D. (1962*a*). A modification of the Hodgkin–Huxley equations applicable to Purkinje fibre action and pace-maker potentials. *J. Physiol.* **160**, 317–352.

NOBLE, D. (1962*b*). The voltage dependence of the cardiac membrane conductance. *Biophys. J.* **2**, 381–393.

NOBLE, D. & HALL, A. E. (1963). The conditions for initiating 'all-or-nothing' repolarization in cardiac muscle. *Biophys. J.* **3**, 261–274.

NOBLE, D. & TSIEN, R. W. (1972). The repolarization process in heart cells. In *Electrical Phenomena in the Heart*, ed. DE MELLO, W. C., pp. 133–161. New York: Academic Press.

PAGE, S. G. & NIEDERGERKE, R. (1972). Structures of physiological interest in the frog heart ventricle. *J. cell Sci.* **11**, 179–203.

SOMMER, J. R. & JOHNSON, E. A. (1969). Cardiac muscle: a comparative ultrastructural study with special reference to frog and chicken hearts. *Z. Zellforsch. nutrosk. Anat.* **98**, 437–468.

STALEY, N. A. & BENSON, E. S. (1968). The ultrastructure of frog ventricular cardiac muscle and its relationship to mechanisms of excitation-contraction coupling. *J. Cell Biol.* **38**, 99–114.

TARR, M. & TRANK, J. (1971). Equivalent circuit of frog atrial tissue as determined by voltage clamp-unclamp experiments. *J. gen. Physiol.* **58**, 511–522.

TASAKI, I. (1956). Initiation and abolition of the action potential of a single node of Ranvier. *J. gen. Physiol.* **39**, 377–395.

VASSALLE, M. (1966). Analysis of cardiac pacemaker potential using a 'voltage clamp' technique. *Am. J. Physiol.* **210**, 1335–1341.

WEIDMANN, S. (1951). Effect of current flow on the membrane potential of cardiac muscle. *J. Physiol.* **115**, 227–236.

WEIDMANN, S. (1956). Shortening of the cardiac action potential due to a brief injection of KCl following onset of activity. *J. Physiol.* **132**, 109–183.